

## Understanding Synthesis Parameters for Thionation of Phosphonates Associated with the Chemical Weapons Convention through Principal Component Analysis

Caio V. N. Borges,<sup>b,\*</sup> Leandro B. Bernardo,<sup>a,b</sup> Samir F. A. Cavalcante<sup>b,c</sup>  
and Antônio L. S. Lima<sup>b,\*</sup>

<sup>a</sup>Instituto Militar de Engenharia (IME), Praça General Tibúrcio, 80, 22290-270 Rio de Janeiro-RJ, Brazil

<sup>b</sup>Instituto de Defesa Química, Biológica, Radiológica e Nuclear (IDQBRN),  
Centro Tecnológico do Exército (CTEx), Avenida das Américas, 28705, Área 4,  
23020-470 Rio de Janeiro-RJ, Brazil

<sup>c</sup>Department of Chemistry, Faculty of Science, University of Hradec Kralove,  
Rokitanskeho 62, 50003, Hradec Kralove, Czech Republic

Thiophosphonates, a class of the organophosphate compounds, are of pharmaceutical and agricultural significance. Albeit their broad scope for peaceful uses, they may also be precursors and markers to toxic chemicals, such as the nerve agent VX and other V-series agents, leading to their inclusion into the Annex as Chemicals of the Chemical Weapons Convention (CWC). Considering that they are related to chemical warfare agents and the position of our laboratory as an Organization for the Prohibition of Chemical Weapons (OPCW) Designated Laboratory for analysis of authentic environmental samples, this study aims to contribute to the understanding of the synthesis of thiophosphonates through *O,O'*-diethyl methylphosphonate conversion to *O,O'*-diethyl methylphosphonothioate using Lawesson's reagent, exploring different conditions previously reported by the literature, in order to further build a compound library for CWC verification purposes. Synthesis of the compounds has been carried out in sealed, pressure tubes, adding novelty to the present study. Reactions were followed by gas chromatography and <sup>31</sup>P nuclear magnetic resonance, and principal component analysis was employed to understand the intricate factors influencing thiophosphonate synthesis yield as duration, temperature and solvent. The research aims to reinforce or challenge existing scientific knowledge, providing insights into parameters related to phosphonate thionation using Lawesson's reagent, contributing to a deeper understanding of this chemical reaction.

**Keywords:** thiophosphonate, principal components analysis, Lawesson's reagent, phosphonate, thionation, chemical weapons convention

### Introduction

Organophosphates hold a crucial and varied significance in the chemical industry, functioning in roles that range from antioxidants to plastic stabilizers, agricultural pesticides, and flame retardants.<sup>1-3</sup> Furthermore, research on organophosphates has gained relevance in the context of international security, particularly concerning chemical weapons.<sup>4,5</sup> The inclusion of these compounds in regulatory lists, such as the Chemical Weapons Convention (CWC), which is overseen by the Organization for the Prohibition of Chemical Weapons (OPCW), underscores the critical

importance of understanding the synthesis, properties, and potential applications of these substances.<sup>5,6</sup> Examples of such toxic chemicals are the nerve agents tabun (1), sarin (2), soman (3), ciclosarin (4), VX (5), VR (6), CVX (7), A230 (8), A242 (9), A262 (10), whose structures are depicted in Figure 1.

Systematic studies on organophosphates date back to around 1820.<sup>7</sup> After a hiatus of nearly 30 years, Thénard and colleagues advanced studies on phosphines,<sup>3</sup> while Clermont synthesized pyrophosphonates, thereby expanding the capability to manipulate reactions related to phosphorus.<sup>3</sup> In the late 19<sup>th</sup> century, Michaelis contributed to the conversion of trivalent phosphorus to pentavalent, and Arbuzov subsequently enhanced this mechanism comprehension.<sup>8</sup> Since then, several research groups

\*e-mail: caiborges.nogueira@ime.eb.br; santoslima@ime.eb.br  
Editor handled this article: Albertina Mogliani (Associate)



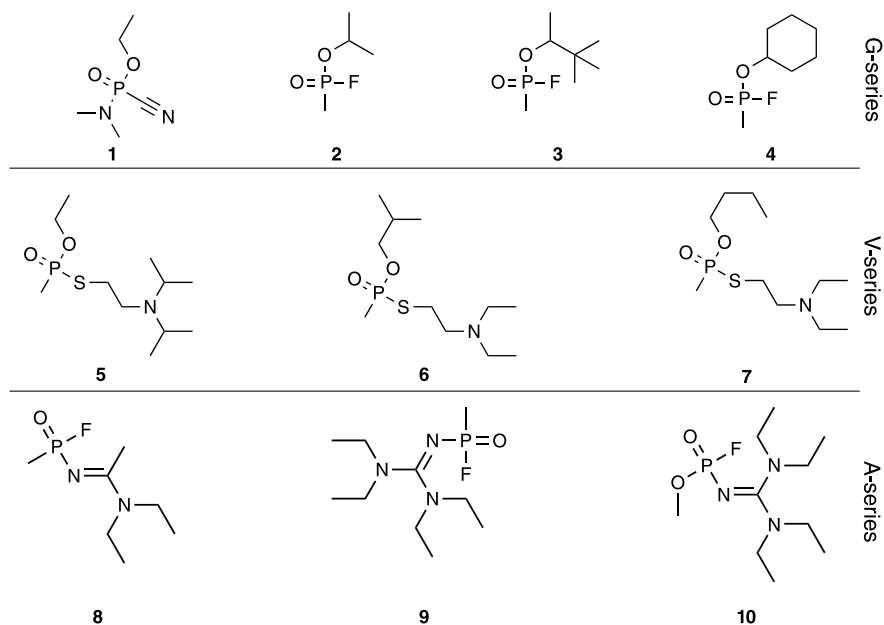


**Figure 1.** Structures of some organophosphorus related in the CWC.

have committed to advancing their understanding of organophosphates.

A subclass of organophosphates is the thiophosphonates, which differ from phosphonates by substituting phosphoryl with thiophosphoryl in their structure, an isosteric substitution of chalcogens oxygen to sulfur. They present pharmaceutical applications as antiviral medication,<sup>8</sup> there is application as a rubber vulcanization acceleration agent,<sup>7</sup> and they are widely used as pesticides (diazinon, malathion, parathion).<sup>9-13</sup> Regardless of their fair use in the chemical industry, these compounds are precursors and relevant markers for the synthesis of V-agents, as VX (5), one of the most potent synthetic toxins. Therefore, they are relevant compounds for the framework of the CWC. For the OPCW roster of Designated Laboratories, the ability to identify their presence and samples and to perform their synthesis, as some of them are not commercially available, are clearly warranted. It is noteworthy that those thiophosphonates with methyl, ethyl, propyl, or isopropyl groups as  $R_1$  are compulsorily listed in the CWC, regardless of any alkylated groups as  $R_2$  and  $R_3$ , as they are potential precursors to the nerve agents. Such broad scope adds complexity to research in that field, leading to the limitation of the study of molecules like those shown in Figure 2 to a few research groups.<sup>14</sup>

The synthesis of thiophosphonates usually proceeds through the formation of thiophosphoryl.<sup>1,15</sup> This conversion of oxygenated groups containing carbonyl or phosphoryl into thiocarbonyl or thiophosphoryl has two predominant approaches in the literature: the use of phosphorus pentasulfide ( $P_4S_{10}$ )<sup>16</sup> or Lawesson's reagent (LR), 2,4-bis(4-methoxyphenyl)-

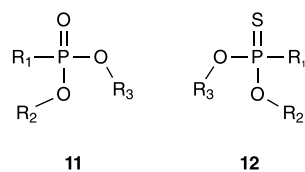


**Figure 2.** General structure of phosphonate (11) and thiophosphonate (12).

1,3,2,4-dithiadiphosphetane-2,4-disulfide (Figure 3).<sup>15,17</sup> A noteworthy aspect in converting the phosphonate into its corresponding thiophosphonate is the potential to achieve this transformation in a single-step synthesis using a commonly employed thionation agent.<sup>16-18</sup>

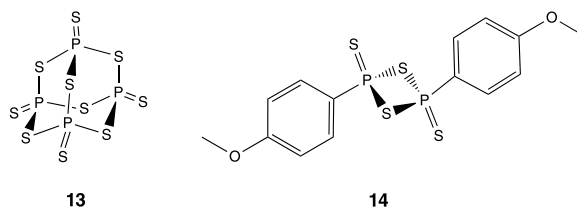


**Figure 3.** Phosphorus pentasulfide (13) and Lawesson's reagent (14).

The synthesis of thiophosphonates can be achieved through LR, which is versatile in the thionation of carbonyls, whether ketones, amides, esters, and phosphonates.<sup>19</sup> Unlike  $P_4S_{10}$ , the literature reports that LR reacts almost equimolarly with a wide variety of carbonylated compounds, eliminating the need for excess. Additionally, LR demonstrates a shorter thionation time compared to  $P_4S_{10}$ , especially when the reaction is microwave-irradiated.<sup>15,20,21</sup> However, LR faces challenges such as solubility difficulties, particularly in low-polarity solvents, and instability at temperatures

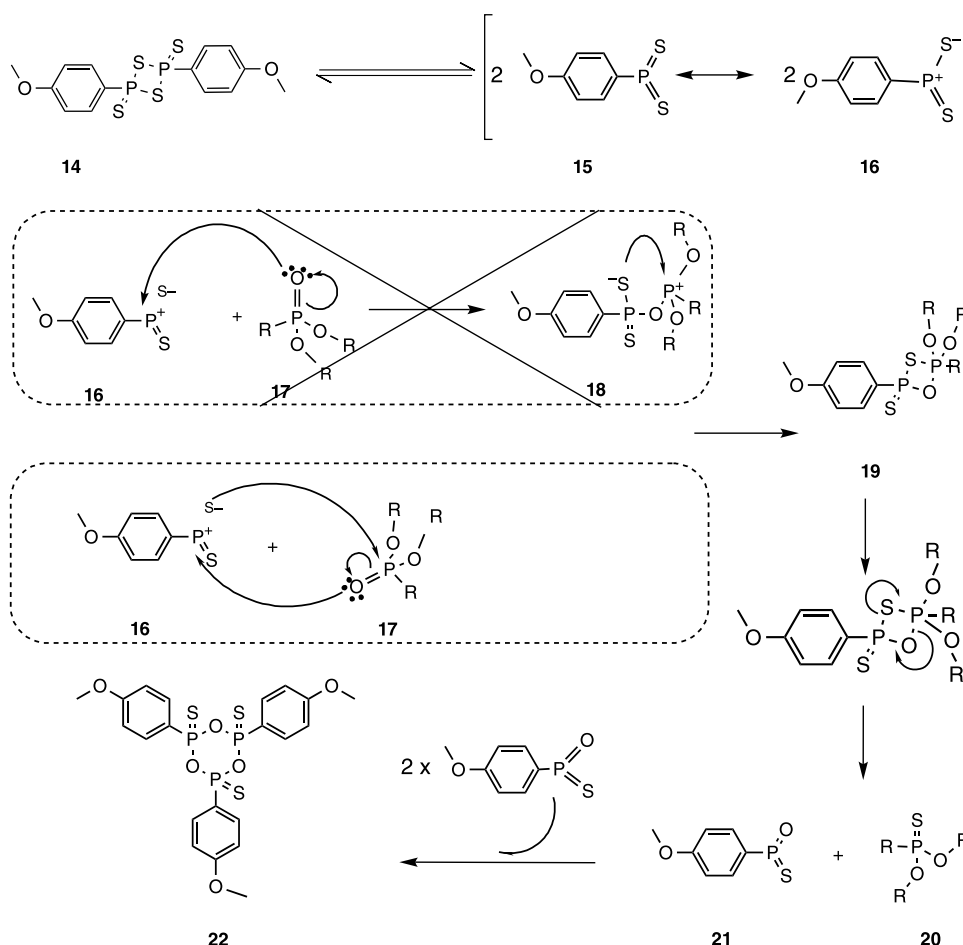
above 110 °C. This contrasts with the robustness of  $P_4S_{10}$ , capable of withstanding temperatures above 150 °C without undergoing decomposition or polymerization reactions.<sup>17,18</sup>

The thionation mechanism using LR follows Scheme 1, which exhibits a considerable mechanistic similarity to the Wittig reaction, including the same paradigms: a mechanism via betaine **18** or [2 + 2]-cycloaddition.<sup>15,17,21-23</sup> It is noteworthy that recent studies, employing molecular modeling in conjunction with the isolation of intermediates, suggest that the initial stage of the reaction does not proceed via nucleophilic attack but rather through a [2 + 2] cycloaddition reaction.<sup>24,25</sup>

When in solution and heated, LR is capable of generating compound (**15**) (dithioxophosphorane) and consequently (**16**), as both contribute to the resonance of the dithiophosphinic ylide, a structure more reactive than LR itself.<sup>23</sup> After the [2 + 2] cycloaddition of compounds (**16**) and (phosphonate), the reaction proceeds through intermediate compound (**19**), a thiaoxaphosphetane, a structure similar again to that occurring in the oxaphosphetane intermediate in the Wittig reaction.<sup>26</sup> Finally, a cycloreversion occurs in compound **19**, generating

compound **21** (oxothiophosphorane) and compound **20**, the thiophosphoryl, this step being slow in the reaction, similar to what occurs in a Wittig reaction for stable ylides.<sup>24,25,27</sup> It is noteworthy the formation of byproduct (**22**), a trimer of thioxophosphane, instead of the dimer, since a state of lower overall energy in the reaction is enabled by the formation of a 6-membered heterocycle, while the dimer would present a more strained cyclic structure.<sup>24,28</sup>

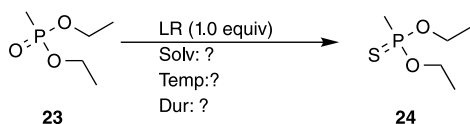
For a better understanding of the factors influencing this reaction, principal component analysis (PCA), a mathematical tool employed to explore numerous variables influencing a specific phenomenon, has been used,<sup>29,30</sup> such as reaction time, temperature, solvent, and the reaction yield. PCA is a technique that performs linear transformations on dependent variables, resulting in uncorrelated latent variables.<sup>31,32</sup> This approach has the advantage of summarizing the information contained in multiple dependent variables into a few latent variables, thus achieving dimensionality reduction.<sup>30,31</sup> Additionally, PCA enables the identification of clusters and similarities among different treatments, providing a multivariate view of the relationships between the studied variables.<sup>32,33</sup> In



**Scheme 1.** Phosphonate thionation mechanism by Lawesson's reagent.

summary, the judicious application of PCA offers a robust approach for analyzing variables in chemical experiments, allowing for a deeper and more efficient understanding of the relationships among the investigated parameters.<sup>31</sup>

This work has specifically focused on the conversion of the *O,O'*-diethyl methylphosphonate (DEMP, **23**) into *O,O'*-diethyl methylphosphonothioate (DEMPS, **24**) using LR (Scheme 2), aiming for a more empirical understanding of how temperature, solvent, and reaction times can interfere with the reaction yield from the perspective of PCA to reinforce the understanding of the process, including conditions considered previously inefficient by the literature. It aims to provide information that corroborates or challenges the established information in the scientific community about this topic.



**Scheme 2.** Investigated reaction by the parameters of solvent, temperature and reaction duration.

## Experimental

### Chemicals

Iodomethane, *N,N*-dimethylformamide, triethyl phosphate, triethylamine, Lawesson's reagent, dichloromethane (DCM), toluene (TOL), acetonitrile (ACN), benzene (BEN) and tetrahydrofuran (THF) were purchased from Sigma-Aldrich (São Paulo, Brazil). Xylene (mixture of isomers) was purchased from Hexágono Química (Rio de Janeiro, Brazil). Deuterated solvent  $\text{CDCl}_3$  containing 1% v/v tetramethylsilane (TMS) as internal standard for  $^1\text{H}$  and  $^{13}\text{C}$  nuclear magnetic resonance (NMR) was purchased from Cambridge Isotopes Laboratories (Tewksbury, Massachusetts, USA). Triphenylphosphate standard for  $^{31}\text{P}$  NMR was acquired from Bruker BioSpin Corporation (Billerica, Massachusetts, USA).

### Materials and equipment

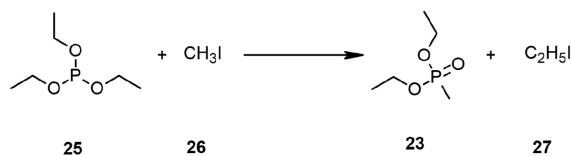
Sealed tubes (Q-Tube) were purchased from Q-Labtech (East Lyme, Connecticut, USA). The NMR spectra were obtained by Bruker Avance III 400 MHz, manufactured by Bruker Corporation (Billerica, Massachusetts, USA). The frequencies for  $^1\text{H}$ ,  $^{13}\text{C}$  and  $^{31}\text{P}$  were 400, 100 and 161 MHz, respectively. Gas chromatography-mass spectrometry (GC-MS) data were acquired from Agilent 7890A GC system (Santa Clara, California, USA) equipped with 5975C mass spectrometer detector.

### Software

Agilent MSD ChemStation E.02.02.1431 was used for GC-MS data acquisition and F.01.00.1903 processing (Agilent Technologies, Santa Clara, California, USA). Bruker TopSpin 4.1.4 was used for NMR experiments (Bruker BioSpin, Billerica, USA). For data analysis, it was used Matlab R2022a (MathWorks, Natick, USA)<sup>34</sup> and Past 4.13 (Palaeontologia Electronica, USA).<sup>35</sup>

### Synthesis of *O,O'*-diethyl methylphosphonate (DEMP)

DEMP was synthesized by a Michaelis-Arbuzov reaction (Scheme 3). Briefly, triethyl phosphite (**25**, 8.6 g, 51.6 mmol, 1 eq.) and iodomethane (**26**, 18.3 g, 128.9 mmol, 2.5 eq.) were added into a 12 mL-Q-Tube equipped with a magnetic stirrer. Then, the system was sealed and heated at 80 °C with the aid of a heating block, with stirring for 24 h. The final mixture was evaporated with a rotary evaporator to remove volatiles (excess of **26** and byproduct iodoethane **27**), affording a colorless oil.



**Scheme 3.** DEMP synthesis (conditions: Q-Tube, 80 °C, 24 h).

### Diethyl methylphosphonate (**23**)

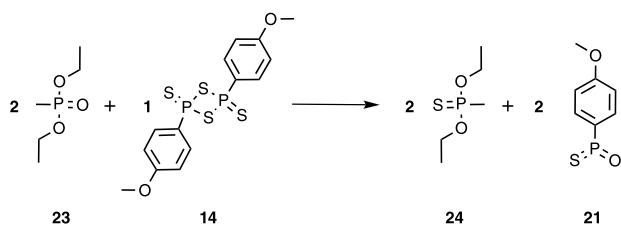
Colorless oil; yield 96%;  $^1\text{H}$  NMR (400 MHz,  $\text{CDCl}_3$ )  $\delta$  4.09 (m, 2H,  $\text{CH}_2$ ), 1.46 (d, 3H,  $J$  17.56 Hz,  $\text{CH}_3$ ), 1.33 (t, 3H,  $J$  7.1 Hz,  $\text{CH}_3$ );  $^{13}\text{C}\{^1\text{H}\}$  NMR (100 MHz,  $\text{CDCl}_3$ )  $\delta$  61.41 (d, 2C,  $J$  6.24 Hz, CP), 16.44 (dd, 2C,  $J$  17.24, 6.23 Hz, CP), 11.77 (dd, 1C,  $J$  144.15, 12.47 Hz, CP);  $^{31}\text{P}\{^1\text{H}\}$  NMR (161 MHz,  $\text{CDCl}_3$ )  $\delta$  29.85; MS (EI)  $m/z$ , 152, 79 [ $\text{M}^+$ ].

## Results and Discussion

The initial range definition for reaction time, temperature and which solvents should be used was based on similar experiments from the literature.<sup>17,36,37</sup> The procedures to thionation were initially the solvent addition (2 mL) to the Q-Tube followed by 76 mg of DEMP and 101 mg of LR, in that order (Scheme 4). The stirrer was put inside the tube and sealed.

Initially, the system was analyzed for each solvent proposed to be evaluated: ACN, THF, TOL, XYL and BEN at 75 °C and analyzing the reactions at the moments of 0, 1, 2, 4, and 24 h under this temperature, as indicated in

Table 1. After this stage, the temperature was increased to 100 °C, and the reaction mixture was left for an additional 24 h under this condition. Finally, the temperature was further increased to 150 °C, and the reaction continued for an additional 5 h. Every yield percentage calculated in this study was determined through quantitative analysis using  $^{31}\text{P}\{^1\text{H}\}$  NMR, and such analyses were performed on the final reaction mixture without any purification process to preserve all quantities of target molecules.



**Scheme 4.** General synthesis of DEMPS under all parameter conditions.

It was observed in the case of THF that there was no variation in the DEMP signal in any chromatogram, suggesting that it remained inert in the mixture. On the other hand, in the ACN reaction, there was a significant decrease in the intensity of the DEMP signal in the chromatogram when the temperature was increased to 150 °C, indicating that this reagent took a parallel synthesis route. The other temperatures did not cause signal reduction for ACN. Both solvents were set aside, and the analysis proceeded exclusively with the aromatic ones.

From a general standpoint, benzene displayed the most favorable characteristics among the three aromatic solvents, particularly in terms of achieving a higher reaction yield. Regarding the formed by-products that can be seen by

**Table 1.** Outcomes of following tests under diverse reaction conditions

Experiment	Solvent	Temperature / °C	Duration / h	Yield / %
1	THF	75-100-150	24-24-5	0
2	ACN	75-100-150	24-24-5	0
3	TOL	75-100-150	24-24-5	20.6
4	XYL	75-100-150	24-24-5	9.6
5	BEN	75-100-150	24-24-5	60.4
6	BEN	90	1	8.0
7	BEN	90	2	13.2
8	BEN	90	4	14.8
9	BEN	120	1	31.0
10	BEN	120	2	28.7
11	BEN	120	4	25.6
12	BEN	120	24	38.9
13	BEN	150	1	24.6
14	BEN	150	2	25.5
15	BEN	150	4	28.5
16	BEN	150	24	81.8

ACN: acetonitrile; THF: tetrahydrofuran; TOL: toluene; XYL: xylene; BEN: benzene.

$^{31}\text{P}$  NMR, it is known that they necessarily originate from either DEMP or LR, as these are the only phosphorus species in the mixture. TOL showed fewer signals in the phosphorus NMR than BEN and XYL, indicating fewer phosphorus-containing by-products (Figure 4).

Another interesting aspect is when comparing Figures 5 and 6 is the total ion chromatogram (TIC) evolution profile of TOL and BEN respectively of DEMP and DEMPS signals while the reaction occurs, indicating how changes

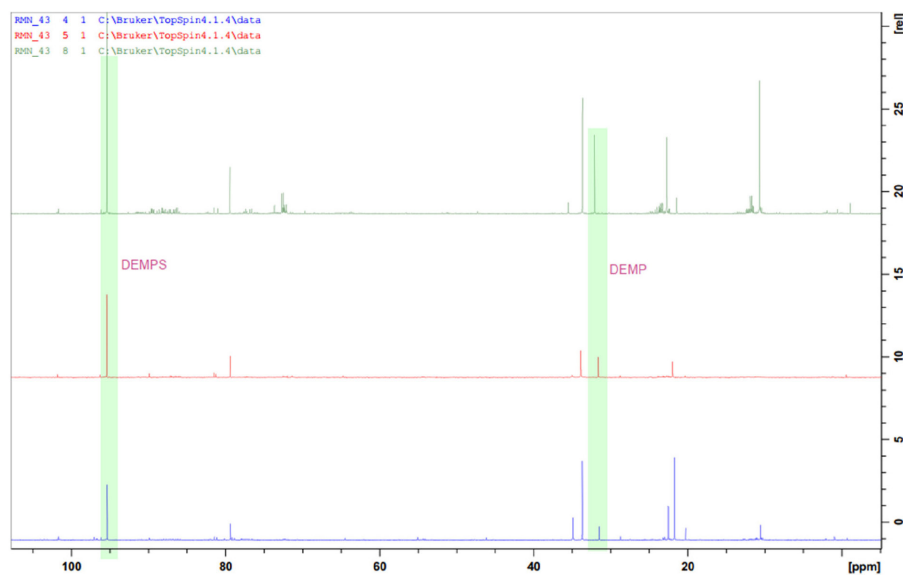


**Figure 4.**  $^{31}\text{P}\{^1\text{H}\}$  NMR spectrum (161 MHz,  $\text{CDCl}_3$ ) at the end of experiments 3, 4 and 5. Blue: xylene, red: toluene, green: benzene. DEMPS and DEMP has a  $\delta$  of 95 and 32 ppm, respectively.

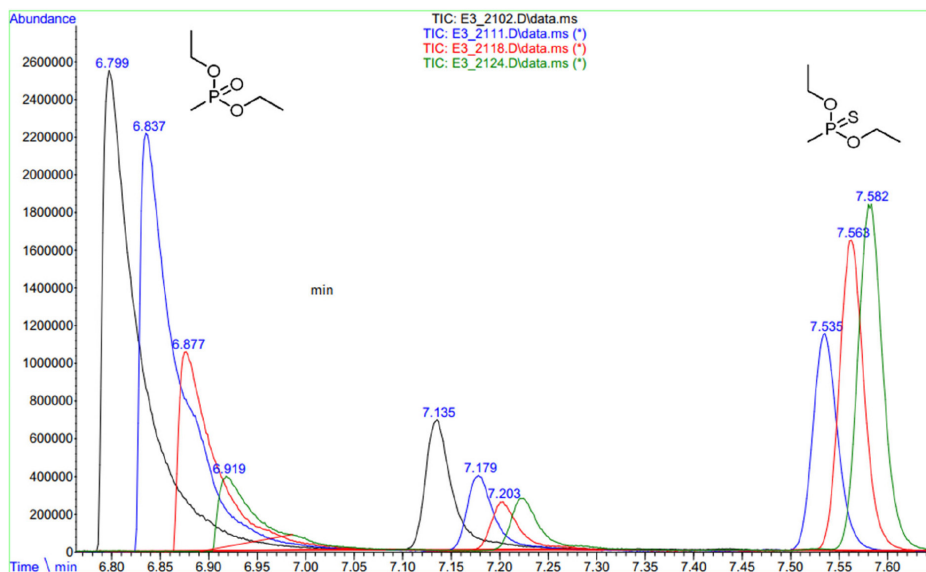


**Figure 5.** TOL experiment: black, blue, red and green TICs are respectively related to the initial moment, 24 h at 75 °C, 24 h at 100 °C, and an additional 5 h at 150 °C.

in temperature and reaction time affect them. It was not possible to create a stacked chromatogram for XYL reaction, due to the signal superposition over the retention time ( $t_R$ ) of DEMP and DEMPS. The reaction in TOL the LR solubilization occurs immediately and shows a more gradual decrease in the amount of DEMP and the appearance of DEMPS, as if each variation in reaction parameters led to better yields, as Figure 5 shows. In contrast, the reaction in BEN proceeded more rapidly, with significant DEMP consumption in the first 24 h.

Analyzing Figure 6, the stacked TICs, it is possible to evaluate that the critical moment for DEMP consumption is within 24 h of reaction, due TO the black signal drop at

$t_R$  6.947 min. The complete solubilization of LR in BEN takes place only when the temperature reaches 100 °C, which corresponds to the red chromatogram and the increment in the DEMPS signal to its maximum.

From this comparison, the temperature increment to 100 °C in both reactions showed a significant reduction in the DEMP signal and an increment in the DEMPS signal, especially in the BEN case. However, the DEMPS signal in BEN declined after the reaction reached 150 °C, while in TOL the signal increased. Upon that and Figure 4, that indicates that the best DEMPS yield was from BEN reaction, even with this chromatographic signal reduction at 150 °C, it can be considered that BEN provides a mixture

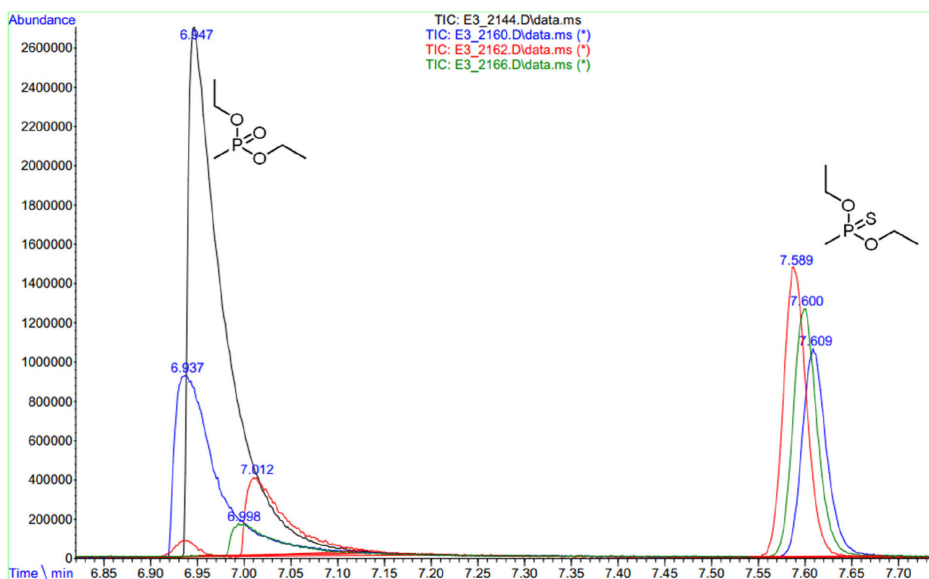


**Figure 6.** BEN experiment: black, blue, red and green TICs are respectively related to the initial moment, 24 h at 75 °C, 24 h at 100 °C, and an additional 5 h at 150 °C.

with the potential to increase the reaction rate especially when kept at temperatures between 100 and 150 °C and the reaction time being inferior to 53 h.

Regarding the purification and cleanup processes, BEN, due to its lower boiling point, becomes the best candidate for rotary evaporation, with less risk of losing reaction products (boiling points > 140 °C), followed by TOL and then XYL (boiling points 80, 110, 138 °C, respectively).

Analyzing from a perspective of solvent polarity effect, the three aromatics are considered nonpolar solvents; nonetheless, benzene is still more polar than toluene, which is more polar than xylene, as methyl groups attached to the aromatic ring reduce the polarity.<sup>38</sup> Additionally, there is still a question regarding the influence of methyl groups in hindering the ability to undergo  $\pi$ - $\pi$  (pi-pi) interaction or pi-stacking between aromatic rings of the solvent and LR.<sup>39</sup> In the specific case of the proposed reaction mechanism, the improved ability of the solvent to stabilize intermediate **19**, a more successful conversion is expected. Therefore, as TOL and XYL have methyl groups that discourage pi-stacking interactions, it might be accounted for the presented outcome.

Given the attributes on Table 2, the solvent that will be subjected to a more thorough scrutiny to establish reaction parameters that provide a higher yield will be benzene. This will involve quantitatively evaluating reaction times at 1, 2, and 4 h for temperatures of 90, 120, and 150 °C. The reaction procedures were maintained in accordance with previous experiments, including the amounts of reagents.

**Table 2.** Comparisons of relevant criteria for choosing the reaction solvent

Solvent	Yield	By-products	Kinetic	Purification
BEN	best	intermediate	best	best
TOL	intermediate	best	intermediate	intermediate
XYL	worst	worst	worst	worst

TOL: toluene; XYL: xylene; BEN: benzene.

For low temperatures (< 90 °C), there were no satisfactory yields; hence, temperatures below 90 °C for the type of reaction in question will be discarded (Figure 7, generated by Matlab).<sup>34</sup> Moving forward in the parameter selection, the best yield was 31% for a temperature of 120 °C for one hour of reaction. However, upon further analysis of the aliquot from the experiment at this temperature, the trend was a reduction in yield. In contrast, for a temperature of 150 °C, the trend was an increase in yield until the last collected moment. Besides, in the experiment 5 yield of 60% was achieved. Considering these two points, it was decided to

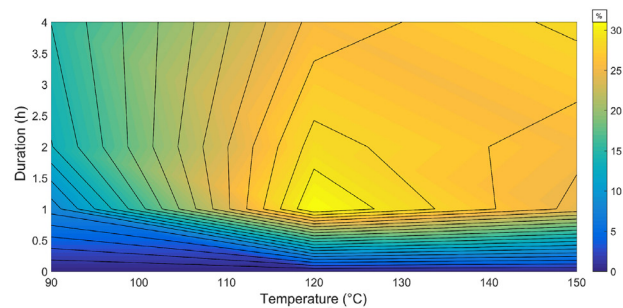


**Figure 7.** Situation 1 yield contour plot.

analyze the aliquots from 120 and 150 °C until the 24 h reaction.

Although there are reports in the literature that temperatures above 110 °C may degrade LR, rendering it ineffective for thionation purposes,<sup>18</sup> the reaction behaved with the best yield precisely at a temperature higher than the established one (Figure 8, generated by Matlab).<sup>34</sup> Another point that differs from the classical LR thionation methodology, which involves refluxing or by microwave reaction,<sup>15,21</sup> all the thionation reactions carried out in this work were conducted in a pressure tube, something not evident in the LR thionation literature, until the present moment.

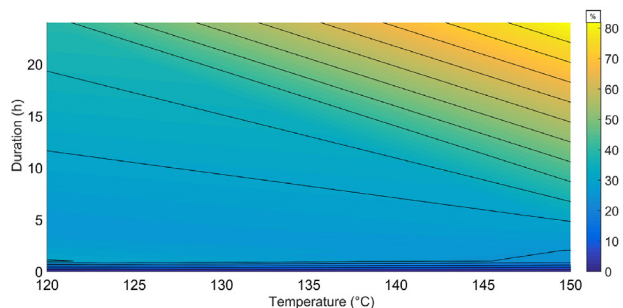


**Figure 8.** Situation 2 yield contour plot.

To extract the maximum information regarding the correlation between the factors temperature (Tem), duration (Dur), and yield (Yie), was used multivariate statistics, specifically through PCA. Data preparation for analysis was performed using the auto-scaling preprocessing method, a procedure based on subtracting each element by the column mean and dividing the result by the standard deviation of the respective column. This mathematical pre-treatment smoothens the discrepancies in variances originating from each variable because, before normalization, the mere difference in variable scales can artificially influence the formation of the principal components to be generated.

Being  $x$  the new matrix of normalized values, it is necessary to determine the matrix of weights and scores  $L$

and T, respectively. In this way, it is established from L the principal components (PCs) relative to the problem, and with T, the new coordinates of the data are defined in the new vector space of the PCs. For this, the singular value decomposition (SVD) method is applied, so that the matrix can be rewritten as equation 2, where U and V are orthogonal matrices, and S is a rectangular matrix with elements off the main diagonal equal to zero.

$$\begin{matrix} \text{Tem} & \text{Dur} & \text{Yie} \\ \left[ \begin{array}{ccc} 90 & 0 & 0 \\ 90 & 1 & 8 \\ 90 & 2 & 13.2 \\ 90 & 4 & 14.8 \\ 120 & 0 & 0 \\ 120 & 13 & 1 \\ 120 & 2 & 28.7 \\ 120 & 4 & 25.6 \\ 120 & 24 & 38.9 \\ 150 & 0 & 0 \\ 150 & 1 & 24.6 \\ 150 & 2 & 25.5 \\ 150 & 4 & 28.5 \\ 150 & 24 & 81.8 \end{array} \right] & \xrightarrow{x_{ij} = (x_{ij} - \bar{x}_j) / s_j} & \begin{matrix} \text{Tem}' & \text{Dur}' & \text{Yie}' \\ \left[ \begin{array}{ccc} -1.2928 & -0.6008 & -1.0816 \\ -1.2928 & -0.4789 & -0.7037 \\ -1.2928 & -0.3570 & -0.4581 \\ -1.2928 & -0.1132 & -0.3826 \\ -0.0862 & -0.6008 & -1.0816 \\ -0.0862 & -0.4789 & 0.3826 \\ -0.0862 & -0.3570 & 0.2739 \\ -0.0862 & -0.1132 & 0.1275 \\ -0.0862 & 2.3247 & 0.7557 \\ 1.1205 & -0.6008 & -1.0816 \\ 1.1205 & -0.4789 & 0.0803 \\ 1.1205 & -0.3570 & 0.1228 \\ 1.1205 & -0.1132 & 0.2645 \\ 1.1205 & 2.3247 & 2.7819 \end{array} \right] \end{matrix} \end{matrix} \quad (1)$$

$$\mathbf{x} = \mathbf{TL}^t = \mathbf{USV}^t \quad (2)$$

When rewriting the data matrix in this new notation, there is an interest in evaluating the matrix V, which is equal to L, and in the matrix S, whose squared values of the main diagonal correspond to the variances. These variances are the eigenvalues associated with the PCs. The importance of these eigenvalues lies in the fact that the amount of original information contained in a single PC is the percentage of the eigenvalue associated with that component divided by the sum of the other eigenvalues.

$$\mathbf{V} = \mathbf{L} = \begin{matrix} & \text{PC}_1 & \text{PC}_2 & \text{PC}_3 \\ \left[ \begin{array}{ccc} 0.4239 & 0.8770 & 0.2262 \\ 0.6129 & -0.4617 & 0.6412 \\ 0.668 & -0.1332 & -0.7333 \end{array} \right] & \begin{matrix} \text{Tem} \\ \text{Dur} \\ \text{Yie} \end{matrix} \end{matrix} \quad (3)$$

$$\mathbf{S}^t \times \mathbf{S} = \mathbf{\Lambda} = \begin{matrix} \left[ \begin{array}{ccc} 26.15 & 0 & 0 \\ 0 & 10.15 & 0 \\ 0 & 0 & 2.2 \end{array} \right] & \xrightarrow{\Lambda_n / \sum_i \Lambda_i} & \mathbf{P} = \begin{matrix} \left[ \begin{array}{c} 67.06\% \\ 27.30\% \\ 5.64\% \end{array} \right] \end{matrix} \end{matrix} \quad (4)$$

Therefore, the 1<sup>st</sup> PC represents a total variance explanation of 67.06%, and the 2<sup>nd</sup> PC presented 27.30%. With only the first two PCs, there is already an explanation of 94.36% of the variance, so the 3<sup>rd</sup> PC will not be computed for the PCA. For the 1<sup>st</sup> PC, the coefficients of greater prominence are related to the factors of duration

and yield. However, since the yield is the response of our system, the interpretation of this coefficient does not make sense for understanding the reaction. Nevertheless, the duration, with a coefficient higher than that of temperature, indicates a higher representativity of this variable for the process within the studied value ranges. In the case of the 2<sup>nd</sup> PC, the temperature variable has the highest representativity in this component.

$$\begin{matrix} & \text{Tem} & \text{Dur} & \text{Yie} \\ \left[ \begin{array}{ccc} 1 & 0.216 & 0.445 \\ 0.216 & 1 & 0.793 \\ 0.445 & 0.793 & 1 \end{array} \right] & \begin{matrix} \text{Tem} \\ \text{Dur} \\ \text{Yie} \end{matrix} \end{matrix} \quad (5)$$

Finally, the correlation matrix (equation 5) still indicates a higher correlation between duration and yield than temperature and yield. It is essential to highlight that these correlations and analyses of PCs are pertinent within the temperature and duration intervals studied, not necessarily reflecting similar behaviors if these limits were exceeded.

$$\text{PC\_COR} = \begin{matrix} & \text{PC}_1 & \text{PC}_2 \\ \left[ \begin{array}{cc} 0.601 & 0.794 \\ 0.869 & -0.418 \\ 0.946 & -0.121 \end{array} \right] & \begin{matrix} \text{Tem}' \\ \text{Dur}' \\ \text{Yie}' \end{matrix} \end{matrix} \quad (6)$$

To assess the correlation between normalized data and PCs scores, a correlation matrix (equation 6) was generated between the original normalized variables and the PCs. The table reveals the characteristics with the strongest correlation to a specific PC, enabling important inferences. The scatter plot analysis illustrates these correlations, where temperature shows a stronger association with PC2 than PC1. Conversely, yield and duration exhibit a stronger correlation with PC1. Thus, higher scores for PC1 correspond to experiments with longer duration and higher yield, while higher PC2 scores indicate higher temperatures. This approach provides a more in-depth understanding of the relationships between the studied variables.

From Figure 9 (generated by Past),<sup>35</sup> points 10, 11, 12, and 13 exhibit higher temperatures than the others, while points 1 to 4 tend to increase along the PC1 axis as the number increases, this suggests that both duration and yield have increased. Points 6, 7, and 8 do not add much information to the interpretation as they represent intermediate values. Notably, points 9 and 14 stand out, implying higher yields and durations, with a higher temperature for point 14 than point 9. Another trend observed is in the direction of the gray arrow, indicating that scores with a negative component of PC2 also presented

PC1 with negative values. With the increase in PC2, there was also an increase in PC1, suggesting that an increase in temperature favors the yield. Finally, it is still possible to add vectors whose coordinates indicate the correlation of the original variables with the PC's, with coordinates as equation 6.

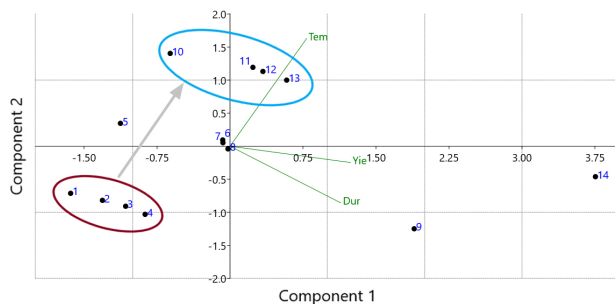


**Figure 9.** PCA scatter plot of components 1 and 2.

## Conclusions

It is possible to highlight the feasibility of conducting thionation using Lawesson's reagent in a pressure tube, an aspect not yet documented. Concerning solvents, the prevalence of aromatic solvents over others was evident. The influence of increasing the reaction duration up to 24 h proved to be more impactful than temperature within the studied range of 75 to 150 °C, particularly regarding yield. As there were no instances of DEMPS decrease during the experiment, it can be concluded that there is no product degradation within the studied intervals. Furthermore, the amount of remaining DEMP at the end of this period suggests that the 2:1 ratio of phosphonate to LR should be changed to equimolar to achieve even higher yields. Through these results, we hope that other research groups can further expand their expertise with this class of compounds and be able to use the information provided by this article to establish the reaction setup for thionation of other phosphonates.

## Supplementary Information

Supplementary information regarding GC-MS and NMR analyses, reaction photographs and graphs are available free of charge at <http://jbcs.sbq.org.br> as PDF file.

## Acknowledgments

Authors would like to thank Brazilian Army, Instituto de Defesa, Química, Biológica, Radiológica e Nuclear (IDQBRN) and Instituto Militar de Engenharia (IME)

for providing the financial support and infrastructure. Additionally, the authors acknowledge Seção de Tecnologias de Materiais de Carbono (SMTC) at Centro Tecnológico do Exército (CTEx) for providing the necessary NMR analyses. C.V.N.B. is also deeply thankful to Prof Dr Jakler Nichele Nunes (IME) for his invaluable advice and contribution of essential resources, which significantly contributed to the progress of this work.

## References

1. He, W.; Hou, X.; Li, X.; Song, L.; Yu, Q.; Wang, Z.; *Tetrahedron* **2017**, *73*, 3133. [Crossref]
2. Swierczek, K.; Peters, J. W.; Hengge, A. C.; *Tetrahedron* **2003**, *59*, 595. [Crossref]
3. *Basic and Clinical Toxicology of Organophosphorus Compounds*; Balali-Mood, M.; Abdollahi, M., eds.; Springer-Verlag London Ltd: Mashhad, Iran, 2014, ch. 1. [Crossref]
4. Barakat, N. H.; Zheng, X.; Gilley, C. B.; MacDonald, M.; Okolotowicz, K.; Cashman, J. R.; Vyas, S.; Beck, J. M.; Hadad, C. M.; Zhang, J.; *Chem. Res. Toxicol.* **2009**, *22*, 1669. [Crossref]
5. Cavalcante, S. F. A.; Simas, A. B. C.; Kuča, K.; *Curr. Org. Chem.* **2019**, *23*, 1539. [Crossref]
6. Franca, T. C. C.; Kitagawa, D. A. S.; Cavalcante, S. F. A.; da Silva, J. A. V.; Nepovimova, E.; Kuca, K.; *Int. J. Mol. Sci.* **2019**, *20*, 1222. [Crossref]
7. Quin, L. D.; *A Guide to Organophosphorus Chemistry*; Wiley: New York, USA, 2000.
8. Corbridge, D. E. C.; *Phosphorus: An Outline of Its Chemistry, Biochemistry, and Technology*, 4<sup>th</sup> ed.; Elsevier: Amsterdam, The Netherlands, 1990.
9. Matula, M.; Kucera, T.; Soukup, O.; Pejchal, J.; *Catalysts* **2020**, *10*, 1365. [Crossref]
10. Zammataro, A.; Santonocito, R.; Pappalardo, A.; Sfrazzetto, G. T.; *Catalysts* **2020**, *10*, 881. [Crossref]
11. Delfino, R. T.; Ribeiro, T. S.; Figueroa-Villar, J. D.; *J. Braz. Chem. Soc.* **2009**, *20*, 407. [Crossref]
12. Valdez, C. A.; Leif, R. N.; *Molecules* **2021**, *26*, 4631. [Crossref]
13. Jakanović, M.; Kosanović, M.; *Environ. Toxicol. Pharmacol.* **2010**, *29*, 195. [Crossref]
14. Vanninen, P. In *Recommended Operating Procedures for Analysis in the Verification of Chemical Disarmament*, 1<sup>st</sup> ed.; Vanninen, P.; Hakulinen, H.; Puustinen, A.; Valtanen, A.; Ginter, J.; Heikkinen, H.; Blake, T., eds.; University of Helsinki: Helsinki, Finland, 2023.
15. Ozturk, T.; Ertas, E.; Mert, O.; *Chem. Rev.* **2007**, *107*, 5210. [Crossref]
16. Ozturk, T.; Ertas, E.; Mert, O.; *Chem. Rev.* **2010**, *110*, 3419. [Crossref]
17. Cava, M. P.; Levinson, M. I.; *Tetrahedron* **1985**, *41*, 5061. [Crossref]

18. Ori, M.; Nishio, T.; *Heterocycles* **2000**, *52*, 111. [Crossref]
19. Wang, J.; Huang, X.; Ni, Z.; Wang, S.; Wu, J.; Pan, Y.; *Green Chem.* **2015**, *17*, 314. [Crossref]
20. Khatoon, H.; Abdulmalek, E.; *Molecules* **2021**, *26*, 6937. [Crossref]
21. Bergman, J.; *Synthesis* **2018**, *50*, 2323. [Crossref]
22. Wang, W.-M.; Liu, L.-J.; Yao, L.; Meng, F.-J.; Sun, Y. M.; Zhao, C.-Q.; Xu, Q.; Han, L.-B.; *J. Org. Chem.* **2016**, *81*, 6843. [Crossref]
23. Yoshifuji, M.; An, D.-L.; Yasunami, M.; *Tetrahedron Lett.* **1994**, *35*, 4379. [Crossref]
24. Legnani, L.; Toma, L.; Caramella, P.; Chiacchio, M. A.; Giofrè, S.; Delso, I.; Tejero, T.; Merino, P.; *J. Org. Chem.* **2016**, *81*, 7733. [Crossref]
25. Robiette, R.; Richardson, J.; Aggarwal, V. K.; Harvey, J. N.; *J. Am. Chem. Soc.* **2006**, *128*, 2394. [Crossref]
26. Byrne, P. A.; Gilheany, D. G.; *Chem. Soc. Rev.* **2013**, *42*, 6670. [Crossref]
27. Abd EL-Rahman, N. M.; Shabana, R.; El-Kateb, A. A.; *Egypt. J. Chem.* **2020**, *63*, 555. [Crossref]
28. Cortés-Santiago, A.; Navarrete-López, A. M.; Vargas, R.; Garza, J.; *J. Phys. Org. Chem.* **2017**, *30*, e3624. [Crossref]
29. Wold, S.; Esbensen, K.; Geladi, P.; *Chemom. Intell. Lab. Syst.* **1987**, *2*, 37. [Crossref]
30. Jolliffe, I. T.; Cadima, J.; *Philos. Trans. R. Soc., A* **2016**, *374*, 20150202. [Crossref]
31. Bro, R.; Smilde, A. K.; *Anal. Methods* **2014**, *6*, 2812. [Crossref]
32. Meglen, R. R.; *Mar. Chem.* **1992**, *39*, 217. [Crossref]
33. Beattie, J. R.; Esmonde-White, F. W. L.; *Appl. Spectrosc.* **2021**, *75*, 361. [Crossref]
34. *Matlab*, version R2022a, The MatWorks Inc.; Natick, MA, USA, 2022.
35. Past, version 4.13; Palaeotologia Electronica; USA, 2023.
36. Gayen, K. S.; Chatterjee, N.; *Asian J. Org. Chem.* **2020**, *9*, 508. [Crossref]
37. Wang, X. L.; Chen, J. X.; Jia, X. S.; Yin, L.; *Synthesis* **2020**, *52*, 141. [Crossref]
38. Reichardt, C.; Welton, T. In *Solvents and Solvent Effects in Organic Chemistry*, 4<sup>th</sup> ed.; Wiley-VCH: Weinheim, Germany, 2010, ch. 7. [Link] accessed in April 2024
39. Dhotel, A.; Chen, Z.; Delbreilh, L.; Youssef, B.; Saiter, J. M.; Tan, L.; *Int. J. Mol. Sci.* **2013**, *14*, 2303. [Crossref]

Submitted: November 27, 2023

Published online: April 9, 2024